Simulation Study of Microstructure of the Amorphous ZnO

Le The Vinh[1(✉)], Nguyen Doan Quoc Anh[1], Vo Hoang Duy[1], Nguyen Kieu Tam[1], Tran Thanh Nam[1], Mai Van Dung[2,3], and Nguyen Manh Tuan[2]

[1] Faculty of Electrical and Electronics Engineering, Ton Duc Thang University, No.19 Nguyen Huu Tho, District 7, Ho Chi Minh City, Vietnam
lethevinh@tdt.edu.vn

[2] Institute of Applied Materials Science, Vietnam Academy of Science and Technology, No. 01 TL29 Street, Thanh Loc Ward, District 12, Ho Chi Minh City, Vietnam

[3] Thu Dau Mot University, No. 6, Tran van on Street, Phu Hoa Ward, Thu Dau Mot City, Binh Duong Province, Vietnam

Abstract. The simulation of microstructure have been done for amorphous zinc oxide by mean of molecular dynamic method. The microstructure has been analyzed through the pair radial distribution function, coordination number and bond-angle distribution. The evolution of changes take under compression has been observed and analyzed. Data obtained are compared with the experimental results. The simulation shows that the major structural changes take place from an tetrahedral network structure at low density to a closed packed like structure at high density which mainly contains also fivefold and sixfold structural units.

Keywords: Computer simulation · Microstructures · Zinc oxide

1 Introduction

The zinc oxide (ZnO) has great properties, such as optical and electrical properties, which are appropriate for an assortment of electronic and optoelectronic applications, for example, varistors, straightforward highpower gadgets, compound sensors, gas sensors, sun based cells, piezoelectric transducers, electroluminescent gadgets and bright laser diodes [1–3]. In applications of ZnO based on such electrical and optical properties, the control and design of the point defect structure, as well as surface and interfacial structures, are keys to optimizing the device performance. The use of homo-junctions requires both p- and n-type doping, but ZnO is known to show a strong n-type preference [2]. Moreover, there exists controversy on the fundamental issues relevant to native defects and unintentional impurities, such as the sources of the n-type conductivity and non-stoichiometry of reduced ZnO. Many experiments have been devoted to the characterization of the native defects and impurities [3–6, 16]. The oxygen-vacancy (VO) defects in amorphous systems have been investigated by a number of authors using different calculations. Hyeon et al. have performed

V.H. Duy et al. (eds.), *AETA 2017 - Recent Advances in Electrical Engineering and Related Sciences: Theory and Application*, Lecture Notes in Electrical Engineering 465,
https://doi.org/10.1007/978-3-319-69814-4_22

first-principles density functional calculations of amorphous indium gallium zinc oxides (a-IGZO) [7].

It is expected that the vast voids in a shapeless strong displays an indistinguishable conduct from an opening, since it can trade its position with neighbor particles. Franker et al. [8] showed that the extensive void in metal–metalloid shapeless combinations assumes the part of an opening if its sweep is more noteworthy than nuclear range. Moreover, many voids can interface with each other shaping a channel, which fills in as a quick dissemination way. For example, it was tentatively demonstrated that the Au polluting influence in shapeless Ge and Pt in undefined Si diffuses at 673–923 K along interstices. Here they could remain for long time in traps with different profundities [9]. Then again, information about voids and void collections can give a basic depiction of undefined structures [10, 11, 13]. The insights of the void conveyance and the 'void tree', comprising of covering voids, were computed in silica models containing 648 particles [7]. An assortment of crystalline inner structures have been broke down by XRD investigation, and amorphous ZnO thin films have been developed on various material substrates by various methods. The properties of amorphous ZnO films structures depend vigorously on the development condition, particularly the substrate materials and temperature. The diverse crystalline surfaces are said to be developed which are seen in the extinguishing procedure of ZnO indistinct movies, and infer that the interior structure changes rely on upon temperature. In the present work, seven amorphous ZnO models with different densities have been constructed and examined in order to give more detailed information about the change in microstructure under the compression.

2 Calculation Method

Molecular dynamic (MD) simulation of ZnO models containing 2000 atoms in the basic cubic cube with periodic boundary conditions is carried out. In this paper the model samples of amorphous ZnO (a-ZnO) was prepared according to the [12]. Interatomic potential is given as:

$$u_{ij}(r) = \frac{z_i z_j e^2}{r} + D_{ij}\left[\{1 - e^{a_{ij}(r-r_0)}\}^2 - 1\right] + \frac{C_{ij}}{r^{12}} \quad (1)$$

Here r denotes the distance between centers of i^{th} and j^{th} ions; z_i and z_j are the charges of i^{th} and j^{th} ions; D_{ij} is the bond dissociation energy, a_{ij} is a function of the slope of potential energy well, and r_o is the equilibrium bond distance. Values $z_1 = +1.2$ and $z_2 = -1.2$ are the charges of Zn and O. The parameters D_{ij}, a_{ij}, r_o *and* C_{ij} are listed in Table 1. Initial configuration of system was obtained by randomly placing all atoms in simulation box. This configuration is heated to 5000 K and treated over 30000 steps using frequent velocity and coordinate scaling. Then, the system is cooled down to 300 K within 20000 steps. Next, system is allowed to reach equilibrium for over 50000 steps without any disturbance. With this system we prepare 9 samples at temperature of 300 K and pressure ranging from 0 to 30 GPa. Each system is equilibrated for 60000 steps. The structural characteristics are calculated by averaging over

1000 last uncorrelated configurations separated by 10 MD steps. Finally, 6 systems of 2000 atoms (1000 Zn and 1000 O) at temperature of 300 K are constructed using the same calculation schedule.

Table 1. The parameters of pair potentials

Pair	D_{ij} *(eV)*	a_{ij} *(Å^{-2})*	r_o *(Å)*	C_{ij} *(eV. Å^{12})*
Zn-O	0.001221	3.150679	2.851850	1.0
O-O	0.042395	1.379316	3.618701	22.0

3 Results and Discussion

Figure 1 showed the calculated partial radial distribution function (pRDF) of Zn-O pair for the present work and data from Ref. [14]. Although there was a small discrepancy around the second peak in the pRDF, we can see that the pRDF agreed well with calculated pRDF in Ref. [14] in terms of shape, position and height of peaks.

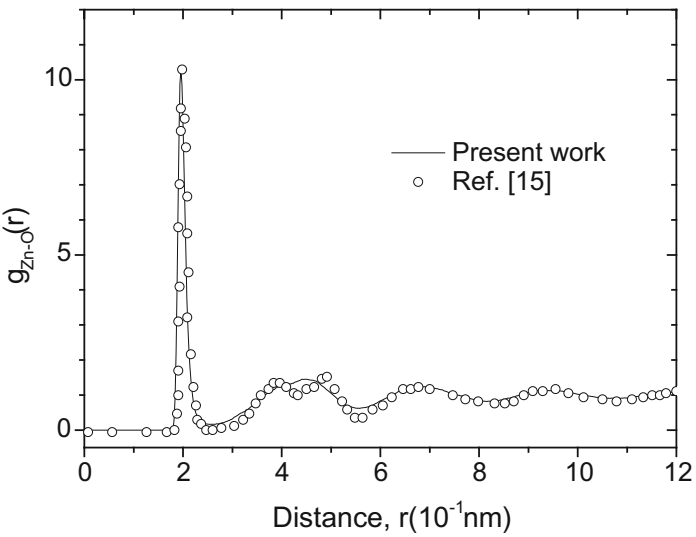

Fig. 1. The partial radial distribution functions (pRDF)

The structural characteristics of obtained models are summarized in Table 2. As mention above, the parameters in this table were obtained by averaging over 1000 configurations. The calculated the bond length between Zn-O is 1.94–1.96 Å for different pressures. This data has the reasonable values and is closed to experimental data in Ref. [15] and simulation data in Ref. [16].

The major change we can notice here is a decrease in the bond length of Zn-Zn, Zn-O and O-O pairs, the height of the first peak of the pRDF, g_{ij}, for the Zn-O pair and

Table 2. Structural characteristics of amorphous ZnO

P, GPa	r_{ij} (Å)			g_{ij}			Z_{ij}		
	Zn-Zn	*Zn-O*	*O-O*	*Zn-Zn*	*Zn-O*	*O-O*	*Zn-Zn*	*Zn-O*	*O-O*
0	3.04	1.96	2.96	1.98	10.28	2.99	13.75	4.11	12.30
5	2.82	1.96	2.90	2.36	9.15	3.46	15.10	4.38	12.98
10	2.78	1.96	2.86	2.54	8.57	3.65	16.16	4.67	13.51
15	2.80	1.96	2.80	2.59	8.54	3.79	16.81	4.88	13.97
20	2.78	1.96	2.80	2.58	8.46	3.69	16.63	4.98	14.30
25	2.74	1.94	2.76	2.39	8.55	3.59	16.23	5.09	14.68
30	2.70	1.94	2.74	2.36	8.77	3.53	15.73	5.18	15.00

an increase in coordination number for the Zn-O, O-O pairs, the height of the first peak of the pRDF, g_{ij}, for the Zn-Zn, O-O pairs as pressure increases.

The change of these structural parameters can be related to the structural transition is very likely to occur.

An overview of simulation on pressure-density relation for temperature 300 K is given in Fig. 2. Note that the curve exhibits the characteristics shape of the liquid equation of state. To get better idea about the averaged coordination numbers (ACN) we show in Fig. 3 the dependence of four-, five- and six-coordinated zinc fractions on pressure. Besides, this maximum occurred at the pressure that corresponds to a point of intersection of the ZnO_4 with ZnO_6 fraction curves (see Fig. 3). The fraction of four-coordinated zinc decreases by 39% as pressure increased from 0 to 10 GPa. In this region of pressure most of the loss of four-coordinated zinc is accounted for by an increase in five-coordinated zinc. Furthermore, whereas pressure increases,

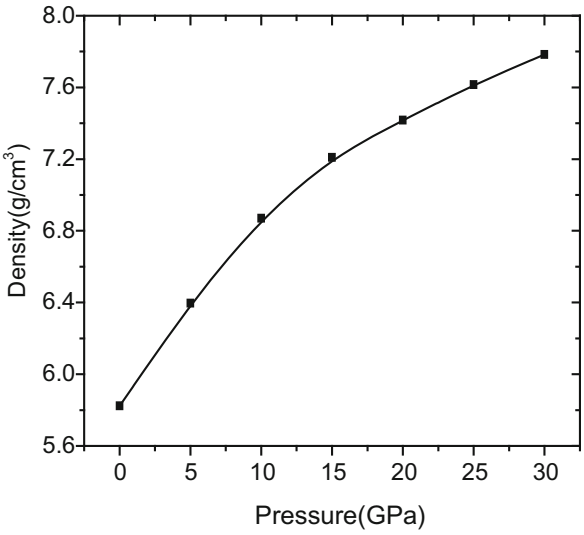

Fig. 2. Density vs. pressure for amorphous zinc oxide at 300 K.

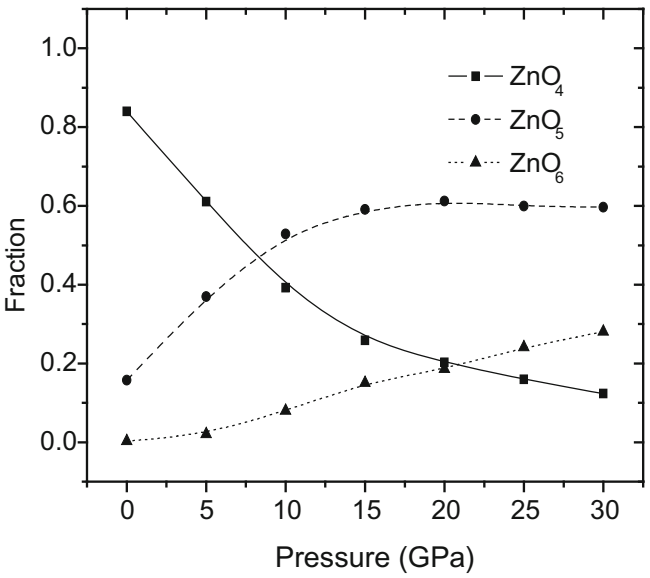

Fig. 3. The dependence of ZnO_4, ZnO_5 and ZnO_6 fractions on pressure for amorphous zinc oxide at 300 K.

the four- and five-coordinated zinc are gradually replaced by six-coordinated zinc. Beyond 30 GPa the percentage of five- and six-coordinated zinc in model reached about 59% and 28% respectively. It mean that at high pressure the elementary structural units of system mainly consist of the octahedrons with the zinc at center and the oxygen in the vertex.

More detail information about basic units can be inferred from the bond-angle distributions. In this work we only calculated most important distribution such as distributions of the O-Zn-O and Zn-O-Zn angles. Fist one describes the short-range order inside structural units, the second provides the connectivity between them. In Fig. 4 we display the angle distributions calculated for three basic units of ZnO_4, ZnO_5 and ZnO_6. For ideal tetrahedron the angle of O-Zn-O is equal to 109.7^0, and In our models the O-Zn-O angle distribution of ZnO_4 has peak at 90^0 that indicated distorted tetrahedral network structure. In the case of five and six-coordinated units both curves has a main peak centered at 85^0 and second peak which occurred near 110^0. It is interestingly that these distributions are almost unchanged with pressure. A little difference observed near main peak in Fig. 4 is related to simulation error. Therefore, as pressure increased, the fraction of structural elementary units such as four, five and six-coordinated zinc changed strongly, but short-range order inside these units are almost unchanged.

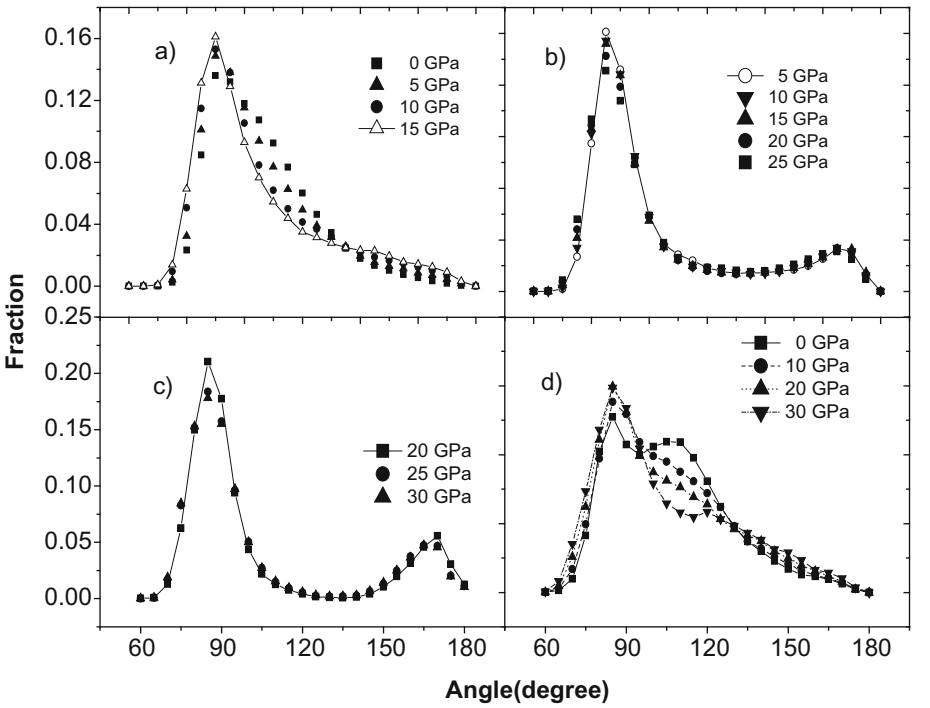

Fig. 4. The angle distribution for amorphous zinc oxide at 300 K. (a) for O-Zn-O in ZnO_4; (b) for O-Zn-O in ZnO_5; (c) for O-Zn-O in ZnO_6 and (d) for Zn-O-Zn in ZnO_x;

4 Conclusion

The MD results for 7 models at different pressure showed that the calculated structures are in good agreement with previous experiment and calculation works. The analysis of systems at different pressure reveals that the major structural changes take place from an tetrahedral network structure at low density to a closed packedlike structure at high density which contains also fivefold and sixfold structural units. At low pressure the two adjacent basic units are linked to each other mainly by corners and also by edges and/or faces as pressure increased. The compression leads to changes in short-range order as well as intermediate-range order described through the O-Zn-O and Zn-O-Zn angle distributions. The changes in short-range order included only the variation in concentrations of structural basic units, and the angle O-Zn-O distributions inside block of ZnO_x are slight change as pressure increased from 0 to 30 GPa. It was found that the region of pressure corresponding to fast dynamic is the one that the maximum in concentration of fivefold zinc versus pressure is compatible to and the point of intersection for ZnO_4 and ZnO_6 fraction curvers is.

Acknowledgment. The authors are grateful for support by the NAFOSTED of Ministry of Science and Technology Vietnam.

References

1. Pearton, S.J., et al.: Recent advances in processing of ZnO. J. Vac. Sci. Technol. B **22**, 932–948 (2004)
2. Tsukazaki, A., et al.: Repeated temperature modulation epitaxy for p-type doping and light-emitting diode based on ZnO. Nat. Mater. **4**, 42 (2005)
3. Allenic, A., et al.: Microstructure and electrical properties of p-type phosphorus-doped ZnO films. Adv. Mater. **19**, 3333 (2007)
4. Ryu, Y.R., et al.: Systhesis of p-type ZnO films. J. Cryst. Growth **216**, 330 (2000)
5. Kim, K.-K., et al.: Realization of p-type ZnO thin films via phosphorous doping and thermal activation of the dopant. Appl. Phys. Lett. **83**, 63 (2003)
6. Noh, H.-K., et al.: Electronic structure of oxygen-vacancy defects in amorphous In-Ga-Zn-O semiconductors. Phys. Rev. B **84**, 115205 (2011)
7. Belashchenko, D.K.: Diffusion mechanisms in disordered systems: computer simulation. Phys. - Uspekhi **42**, 297 (1999)
8. Frank, W., Gustin, W., Horz, M.: Liquid and Amorphous Metals Ninth International Conference Chicago, USA, p. 75, 27 August–1 September 1995
9. Elliott, S.R.: Origin of the first sharp diffraction peak in the structure factor of covalent glasses. Phys. Rev. Lett. **67**, 711 (1991)
10. Sadigh, B., Dzugutov, M., Elliott, S.R.: Vacancy ordering and medium-range structure in a simple monatomic liquid. Phys. Rev. B **59**, 1 (1999)
11. Taraskin, S.N., Elliott, S.R., Klinger, M.I.: Void structure in models of vitreous silica. J. Non-Cryst. Solids **263**, 192 (1995)
12. Pedone, A., et al.: A new self-consistent empirical interatomic potential model for oxides, silicates, and silica-based glasses. J. Phys. Chem. B **110**, 11780 (2006)
13. Vinh, L.T., et al.: Local microstructure of silica glass. J. Non-Cryst. Solids **355**, 1215 (2009)
14. Roy, A., et al.: Amorphous ZnO-based compounds as thermoelectrics. J. Phys. Chem. C **120**, 2529–2535 (2016). https://doi.org/10.1021/acs.jpcc.5b11618
15. Srivastava, A.K., et al.: Structural determination of Zn-O dumbbells in facetted nano-particles. Microsc. Sci. Technol. Appl. Educ. **3**, 1820 (2010)
16. Erhart, P., Klein, A., Albe, K.: First-principles study of the structure and stability of oxygen defects in zinc oxide. Phys. Rev. B **72**, 085213 (2005)
17. Oba, F., et al.: Point defects in ZnO: an approach from first principles. Sci. Technol. Adv. Mater. **12**, 034302 (2011)